Separation Science and Technology
Publication details, including instructions for authors and subscription information:
http://www.informaworld.com/smpp/title~content=t713708471

Energy Consumption and Its Reduction in the Hydrocyclone Separation Process. III. Effect of the Structure of Flow Field on Energy Consumption and Energy Saving Principles

Liang-Yin Chu[ab]; Jian-Jun Qin[a]; Wen-Mei Chen[a]; Xiao-Zhong Lee[a]
[a] SCHOOL OF CHEMICAL ENGINEERING, SICHUAN UNIVERSITY, CHENGDU, SICHUAN, PEOPLE'S REPUBLIC OF CHINA [b] Nakao Laboratory, Department of Chemical System Engineering, School of Engineering, The University of Tokyo, Tokyo, Japan

Online publication date: 19 December 2000

To cite this Article Chu, Liang-Yin , Qin, Jian-Jun , Chen, Wen-Mei and Lee, Xiao-Zhong(2000) 'Energy Consumption and Its Reduction in the Hydrocyclone Separation Process. III. Effect of the Structure of Flow Field on Energy Consumption and Energy Saving Principles', Separation Science and Technology, 35: 16, 2679 — 2705
To link to this Article: DOI: 10.1081/SS-100102363
URL: http://dx.doi.org/10.1081/SS-100102363

SEPARATION SCIENCE AND TECHNOLOGY, **35**(16), pp. 2679–2705, 2000

Energy Consumption and Its Reduction in the Hydrocyclone Separation Process. III. Effect of the Structure of Flow Field on Energy Consumption and Energy Saving Principles

LIANG-YIN CHU,* JIAN-JUN QIN, WEN-MEI CHEN, and XIAO-ZHONG LEE
SCHOOL OF CHEMICAL ENGINEERING
SICHUAN UNIVERSITY
CHENGDU, SICHUAN, 610065, PEOPLE'S REPUBLIC OF CHINA

ABSTRACT

The effect of the structure of flow field in the hydrocyclone on energy consumption was experimentally studied systematically with orthogonal design. The results show that the effect of the inserted central part on energy consumption is the largest, while that of the underflow pipe is the least. The energy saving performance of the winged core is the best among the inserted central parts. The time-averaged and fluctuating characteristics of pressure structure in the hydrocyclone with low energy loss were also investigated experimentally. Both the time-averaged and fluctuating characteristics of pressure structure in the hydrocyclone with low energy loss are much different from those in the conventional commercial hydrocyclone. The energy saving mechanism was investigated, and the energy saving principles and relevant measures for hydrocyclones were proposed systematically.

Key Words. Hydrocyclone; Energy consumption; Energy saving; Structure of fluid flow; Turbulence; Pressure distribution

* To whom correspondence should be addressed before September 2001. Nakao Laboratory, Department of Chemical System Engineering, School of Engineering, The University of Tokyo, 7-3-1 Hongo, Bunkyo-ku, Tokyo 113-8656, Japan. E-mail: chu@nakao1.t.u-toyko.ac.jp

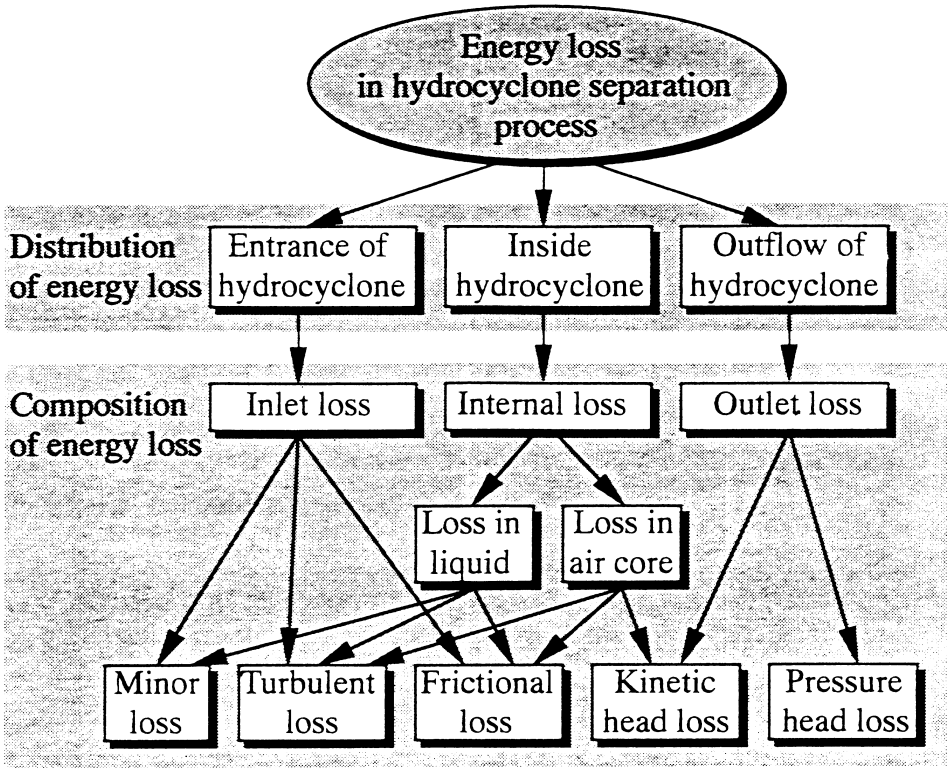

FIG. 1 The energy consumption system in the conventional hydrocyclone separation process.

INTRODUCTION

After the turbulent pressure structure and energy consumption inside the conventional hydrocyclone were studied by means of theoretical investigation (1), numerical simulation (2), and experimental study (3), the general picture of the distribution and composition of energy loss in the conventional hydrocyclone separation process was obtained, as shown in Fig. 1.

In this paper, the investigation focused on the energy saving principles and measures. The results shown in the investigations (1–3) indicated that controlling certain characteristics of the structure of turbulent flow field would effectively reduce the energy loss in the hydrocyclone. Therefore, the effect of the structure of flow field on energy consumption inside hydrocyclones was studied systematically, and then the energy saving principles and relevant measures were determined.

EXPERIMENTAL METHODS

Apparatus

To investigate the effect of the structure of flow field on energy consumption, the structure of flow field in hydrocyclones was changed to match the

conventional hydrocyclone illustrated in the literature (3). The change of the structure of flow field resulted from the variation of boundary conditions of the hydrocyclone. Because many studies have been performed on the dimension scale of the hydrocyclone, the investigation in this paper did not concern the variation of dimension scale, but focused on the variation of the characteristics of boundary conditions of the hydrocyclone. In this study, the following geometric parameters were always kept the same as those of the conventional hydrocyclone used in the literature (3): (*a*) The hydrocyclone diameter, (*b*) the area-equivalent diameter of inlet, (*c*) the diameter of vortex finder, (*d*) the length of vortex finder, (*e*) the diameter of underflow pipe, and (*f*) the length of cone part. The variation of the characteristics of boundary conditions mainly included that of the inlet, vortex finder, cone part, underflow pipe, cylindrical part, and the central area near the hydrocyclone axis.

The Inlet Geometry (A)

To change the structure of flow field in and near the inlet, the variations of inlet geometry include the variation of cross-sectional shape of inlet and the variation of connection pattern between inlet and hydrocyclone body. Five inlet designs are shown in Fig. 2 and Table 1. All of the inlets had the same area-equivalent diameters. The diameters of the round cross-sections were 20 mm, the longer sides of the rectangular cross-sections were parallel to hydrocyclone axis with lengths of 29.92 mm, and the lengths of the shorter sides were 10.5 mm. The slanting angle in type A4 was 20°.

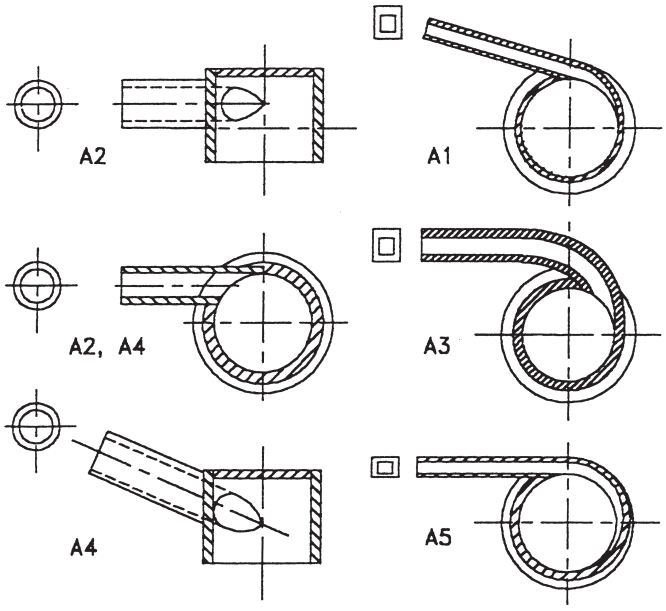

FIG. 2 Schematic diagram of the inlet pipes.

TABLE 1
Design of the Boundary Conditions

Structural factors		Level	
Label	Name	1	2
A	Inlet pipes	Involute type	Tangent type
B	Vortex finders	Straight pipe with thin wall	Straight pipe with thick wall
C	Cone parts	Parabola type	Hyperbola type
D	Underflow pipes	Straight pipe	20° diffuser
E	Central inserted parts	Without inserted part	Solid core
F	Length of cylindrical part	0.4 D	0.8 D

The Vortex Finder (B)

Five designs of the vortex finder are illustrated in Fig. 3 and Table 1. All of the entrance diameters were 25 mm, and all of the lengths were 125 mm. The wall thickness of the vortex finder in type B1 was 2.5 mm, and that in type B2 was 7.5 mm. The design of the annular teeth in type B4 was according to previous investigations (4, 5), and the ratio of the outer diameter of the annular teeth to hydrocyclone diameter was 0.67. In type B5, a siphon device was connected with the outlet of the vortex finder and the siphonage was equal to the water column with height of 1200 mm.

The Cone (C)

The designs of the cone parts are given in Fig. 4 and Table 1. The lengths and the inner diameters of both larger ends and smaller ends of all the cone parts were the same. In type C5, the inner diameters of the larger end and smaller end were 75 and 12.5 mm, respectively, with a cone angle of 20°. In

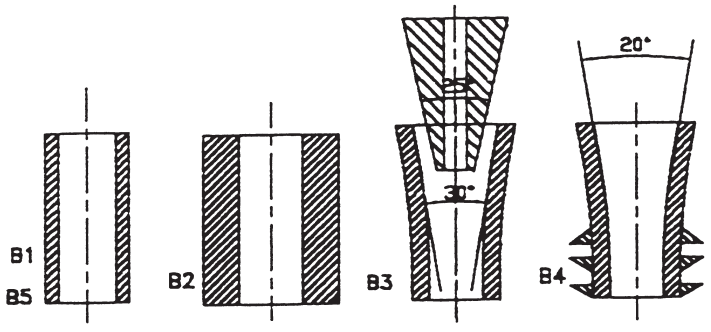

FIG. 3 Schematic diagram of the vortex finders.

of the Hydrocyclones

3	4	5
Arc type	Slanting pipe	Spiral type
30° diffuser plus cone	20° diffuser plus annular teeth	Straight pipe with thin wall plus siphon
20° cone with spiral	20° cone with rings	20° cone with smooth surface
30° diffuser plus cone	Straight pipe plus cone	Straight pipe plus water-sealed tank
Central cone	Inner diffuser	Winged core
1.2 D	1.6 D	2.0 D

type C4, the height of the rings was 3 mm, the width was 5 mm, and the axial distance between the rings was 25 mm. In type C3, the spiral angle was 20°, and with the same spiral direction as that of the outer helical flow in the hydrocyclone. The height of the spiral was 3 mm, and the width was 5 mm. In type C2, the generatrix equation was described as follows:

$$Z = 1259.58r^{-0.1} - 876.67 \quad (1)$$

where the coordinate center was at the center of the larger end of the cone; Z is the axial position in millimiters, and r designates the radial position in millimeters.

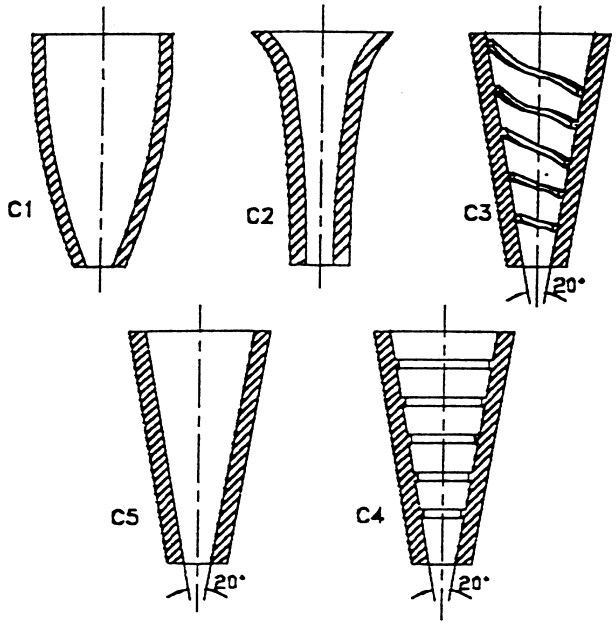

FIG. 4 Schematic diagram of the cone parts.

In type C1, the equation of the generatrix was described as

$$Z = 0.003277r^3 - 0.8 \quad (2)$$

where the coordinate center was chosen at the center of the smaller end of the cone.

The Underflow Pipe (D)

The designs of underflow pipes are shown in Fig. 5 and Table 1. All of the underflow pipe lengths were 60 mm, and all of the inner diameters of the entrances of underflow pipes were kept as 12.5 mm. Type D1 was the underflow pipe used in the conventional hydrocyclone (3). In type D5, a kind of water-sealed tank was installed outside the straight underflow pipe.

The Central Inserted Parts (E)

The previous investigations (1–3) showed repeatedly that controlling the structure of flow field in the central area was important to reduce the energy consumption in the hydrocyclone. Therefore, some central inserted parts were designed to change the structure of flow field in the central area inside hydrocyclones. The designs of central inserted parts are given in Fig. 6 and Table 1. Because all of the central inserted parts need to be located and fixed, a kind of thin wire was introduced. The diameter of the wire was experimentally selected as 4 mm under the presupposition that the insertion of the thin wire has no obvious effect on the shape, size, and rocking condition of the air core in hydrocyclones. To let the comparability of experimental results be more convincing, the thin wire was also fixed inside the hydrocyclone to balance the effect of the existence of thin wire when no central inserted parts were introduced. The same consideration was also taken in the

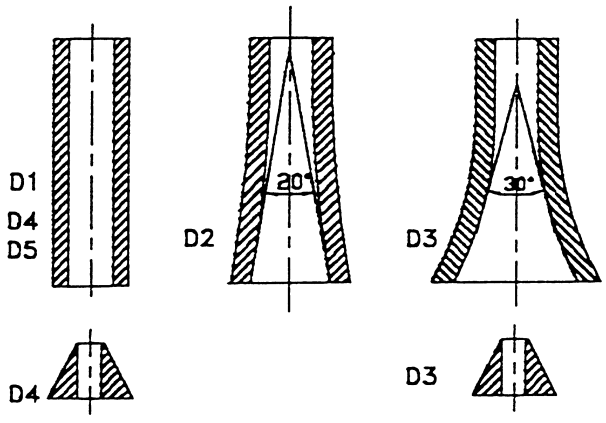

FIG. 5 Schematic diagram of the underflow pipes.

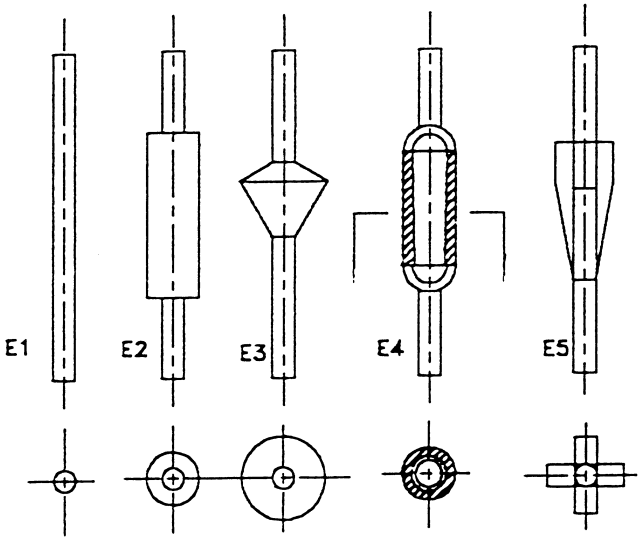

FIG. 6 Schematic diagram of the central inserted parts.

hydrocyclone used in the literature (3). In Fig. 6, type E1 was the thin wire without the inserted part.

The solid core shown as type E2 was designed according to the literature (6). The ratio of the diameter of the solid core to the inner diameter of the vortex finder entrance was 0.56. The upper end of the solid core was inserted into the vortex finder, and the lower end was above the entrance of the underflow pipe with axial distance of 40 mm. In type E3, the upper cone angle and lower cone angle of the central cone were 120° and 60°, respectively, and the diameter ratio of the larger end of the central cone to the hydrocyclone was 0.41; the larger end was located below the entrance of the vortex finder, with an axial distance of 15 mm. The length of the inner diffuser illustrated as type E4 was 50 mm, the outer diameter was 14 mm, the inner diameter of the upper larger end was 10 mm, and that of the smaller end was 6 mm. The inner diffuser was inserted into the vortex finder, and the smaller end was located above the entrance of the vortex finder with an axial distance of 5 mm. In type E5, the thickness of the wing was 4 mm, and the smallest angle of the right triangle part of the wing was 10°, which was the same as the semiangle of the cone part of the hydrocyclone. The radial width from the axis of the wing was 15 mm. The axial length of the rectangle part of the wing varies with the length of cylindrical part of the hydrocyclone, which allows the upper end of the wing to be located at the horizontal level where the entrance of the vortex finder exists. When the length of cylindrical part of the hydrocyclone is smaller than that of the vortex finder, the axial length of the rectangle part of the wing will be zero.

The Cylindrical Part (F)

The variation of the cylindrical part of the hydrocyclone was mainly related to the length. The parameter designs are shown in Table 1.

Program

To scientifically design the experiments, orthogonal design method (7) was adopted. The labels of the structural factors and levels of the hydrocyclone are given in Table 1. From Table 1, a conventional hydrocyclone with code A2-B1-C5-D1-E1-F4 could be designed. This is the same hydrocyclone as that used in the previous experimental investigation (3).

The design of the experiments in this study was according to the orthogonal design table $L_{25}(5^6)$. The combinations of the structural factors and the levels are shown in Table 2.

TABLE 2
Orthogonal Design Table L_{25} (5^6)

	Structural factors (Level)					
Experiment number	A	B	C	D	E	F
1	1	1	1	1	1	1
2	1	2	2	2	2	2
3	1	3	3	3	3	3
4	1	4	4	4	4	4
5	1	5	5	5	5	5
6	2	1	2	3	4	5
7	2	2	3	4	5	1
8	2	3	4	5	1	2
9	2	4	5	1	2	3
10	2	5	1	2	3	4
11	3	1	3	5	2	4
12	3	2	4	1	3	5
13	3	3	5	2	4	1
14	3	4	1	3	5	2
15	3	5	2	4	1	3
16	4	1	4	2	5	3
17	4	2	5	3	1	4
18	4	3	1	4	2	5
19	4	4	2	5	3	1
20	4	5	3	1	4	2
21	5	1	5	4	3	2
22	5	2	1	5	4	3
23	5	3	2	1	5	4
24	5	4	3	2	1	5
25	5	5	4	3	2	1

In all of the experiments, the inlet pressures were always maintained at 0.08 MPa.

RESULTS AND DISCUSSION

Effects of Structure of Flow Field on Energy Consumption

Definition of the Energy Loss Coefficient

The energy loss in the hydrocyclone separation process is composed of inlet loss, internal loss, and outlet loss, as shown in Fig. 1. The energy loss coefficient of hydrocyclone is defined as the ratio of overall energy loss to the inlet kinetic energy by referring to the concept of loss coefficient in fluid mechanics (8), i.e.:

$$K = \frac{(P_e - 0)/\rho g}{v_e^2/2g} = \frac{P_e}{\rho v_e^2/2} = (\mathrm{Eu})_e \tag{3}$$

where K is the energy loss coefficient; P_e is the inlet pressure; ρ is the density of liquid; v_e is the inlet velocity of liquid; g is the gravitational acceleration; and $(\mathrm{Eu})_e$ stands for the inlet characteristic Euler number.

Equation (3) shows that the energy loss coefficient defined above is physically the inlet characteristic Euler number. The larger the coefficient K, the more energy is consumed.

The hydrocyclone characteristic numbers used to be described with a hydrocyclone characteristic velocity (9), e.g.:

$$(\mathrm{Re})_c = \frac{\rho D v}{\mu}, \qquad (\mathrm{Eu})_c = \frac{P_e}{\rho v^2/2}, \qquad (\mathrm{Fr})_c = \frac{v^2}{Dg} \tag{4}$$

where $(\mathrm{Re})_c$ is the cyclone characteristic Reynolds number; $(\mathrm{Eu})_c$ is the cyclone characteristic Euler number; $(\mathrm{Fr})_c$ is the cyclone characteristic Froude number; D is the hydrocyclone diameter; ρ and μ are the density and viscosity of liquid, respectively; and v is the hydrocyclone characteristic velocity with formula:

$$v = \frac{4Q_e}{\pi D^2} \tag{5}$$

where Q_e is the capacity of hydrocyclone.

The relationships between the energy loss coefficient and the cyclone characteristic numbers could be described as follows:

$$K = \left(\frac{d_e}{D}\right)^4 (\mathrm{Eu})_c \tag{6}$$

$$K = \left(\frac{2\rho P_e d_e^4}{\mu^2 D^2}\right)(\mathrm{Re})_c^{-2} \tag{7}$$

$$K = \left(\frac{2P_e d_e^4}{\rho g D^5}\right)(\mathrm{Fr})_c^{-1} \tag{8}$$

where d_e is the inlet diameter.

Effects of the Structures of Flow Field on Energy Consumption

The orthogonal analysis of the effect of flow field structure on the energy loss coefficient is shown in Fig. 7. According to the degree of influence on the energy loss coefficient, the structural factors could be put in the following order: central inserted parts > inlet pipes > cylindrical parts > vortex finders > cone parts > underflow pipes. The central inserted parts influence the energy loss coefficient most, whereas the degree of effect of the underflow pipes on the energy loss coefficient is the smallest.

To investigate the influences of structural factors on the energy loss coefficient, the structural factors and levels adopted in the hydrocyclone used in the literature (3) are chosen as the basic group for the comparison. The structural combination code of the basic group is A2-B1-C5-D1-E1-F4. The comparison is carried out in each structural factor group individually. For example, in the inlet pipe group, the geometric coefficient of A2 is set as 1.00. Therefore, the geometric coefficient for the energy loss coefficient of A1 is the energy loss coefficient ratio of A1 to A2, and the geometric coefficient of A3 is the energy loss coefficient ratio of A3 to A2. Then, the rest of the comparison is con-

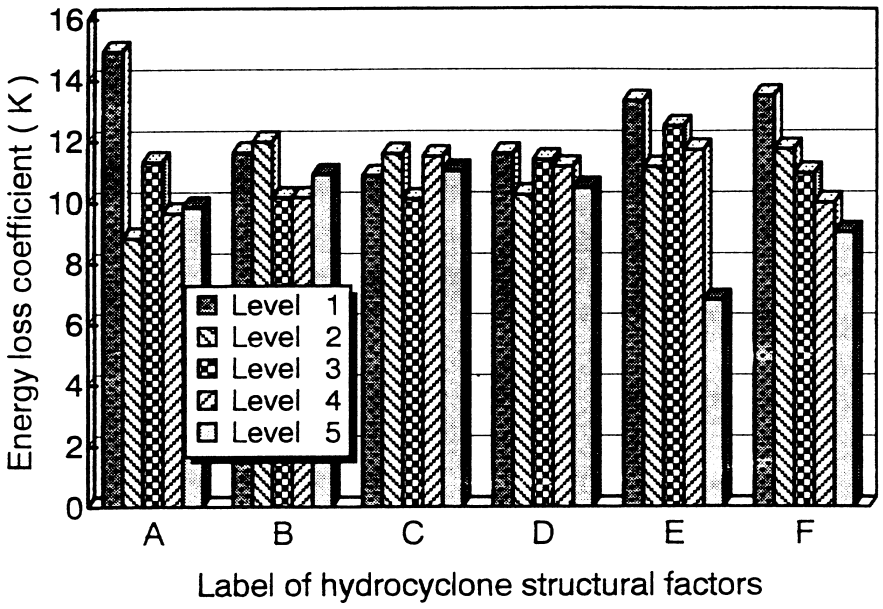

FIG. 7 Effects of hydrocyclone structural factors on the energy loss coefficient.

TABLE 3
Geometric Coefficient for the Energy Loss Coefficient

	Structural factor					
Level	A	B	C	D	E	F
1	1.69	•1.00	0.99	•1.00	•1.00	1.35
2	•1.00	1.03	1.05	0.88	0.84	1.17
3	1.28	0.87	0.92	0.98	0.94	1.10
4	1.09	0.87	1.04	0.96	0.88	•1.00
5	1.11	0.94	•1.00	0.90	0.51	0.90

[a] Bullets refer to the basic group for comparison.

cluded by analogy. The geometric coefficient for the energy loss coefficient is shown in Table 3. Physically, the geometric coefficient shows the variation of energy loss coefficient changing with the levels of structural factor when the traditional commercial levels are used as the basis for comparison. When a geometric coefficient is larger than 1.00, the related energy loss coefficient is larger than that of the related basic level, and vice versa. However, if two or more structural factors vary simultaneously, the overall geometric coefficient of the hydrocyclone cannot be derived by simply multiplying the individual geometric coefficients, because the effects of structural factors on the flow field in hydrocyclones are complicated and nonlinear. Therefore, the comparison of the geometric coefficient could only be carried out in each structural factor group.

The results shown in Fig. 7 and Table 3 illustrate that all of the energy loss coefficients of hydrocyclones with central inserted parts are smaller than that of the hydrocyclone without an inserted part. Compared with the energy loss coefficient of the hydrocyclone without inserted part, the energy loss coefficient of the hydrocyclone with central solid core decreases 16%, that with central cone decreases 6%, that with central inner diffuser decreases 12%, and that with central winged core decreases 49%.

The reason the energy loss coefficient decreases so much when the winged core is introduced as the central inserted part is explained mainly by the following three aspects. First, the winged core has a function similar to that of the large eddy break-up device (10, 11). Most investigations on the flow field inside hydrocyclones have verified that the motion of the central air core and the nearby liquid in conventional hydrocyclones is in a state of forced vortex (12). Falco's investigation (11) shows that the energy transportation and frictional dissipation in the large eddy are the main manner of turbulence energy consumption, and that the introduction of a device to break up the large eddy could cause the energy loss to decrease. The central winged core could break

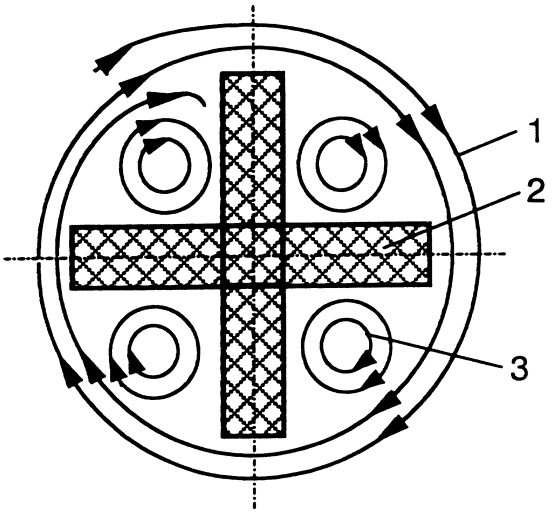

FIG. 8 Flow pattern in and around the winged core: (1) outside helical flow; (2) winged core; (3) inside helical flow.

up the large forced vortex inside the hydrocyclone, as shown is Fig. 8. Experiments with tracer dye show that the large forced vortex is broken up into smaller eddies by the central winged core, i.e., the structure of turbulence is effectively changed, and from which the reduction of turbulent energy consumptionresults.

Second, the central winged core restrains the sharp increase of the liquid velocity in the inner helical flow around the hydrocyclone axis, and then restrains the fast transition between the kinetic energy and pressure head; therefore, the pressure head loss is controlled. Furthermore, because the existence of the central winged core results in effective control of the tangential velocity of the liquid in the inner helical flow, the kinetic head loss within the outlet flow could be reduced; consequently, the overall energy loss is reduced.

Third, the insertion of the winged core eliminates the air core, cancels the energy consumption in the air core, and then decreases the energy loss coefficient.

The experimental results on the inlet pipes (Fig. 7 and Table 3), are somewhat unexpected. The data show that the energy loss coefficient of the hydrocyclone with tangent type inlet pipe is the smallest, whereas when involute, arc, slanting, or spiral type pipes are introduced as the inlet pipe, the energy loss coefficients all increase to some extent. Some previous investigations (13–15) indicated that the inlet energy loss would decrease when the tangent type inlet pipe was replaced by involute, arc, or spiral type pipe. These results need to be reconsidered from the overall point of view. The geometric variation of the inlet pipe influences not only the fluid flow structure at the entrance

of the hydrocyclone, but also the fluid flow structure inside the cylindrical part or even inside the cone part of the hydrocyclone. The disadvantage of involute arc, and spiral types of inlet pipe is that the inlet pipe still has fairly strong directional guidance after guiding the liquid into the hydrocyclone. The surplus directional guidance makes the liquid move in a circular motion, and then the circular motion must be changed into helical motion to fit in the fluid flow pattern inside the hydrocyclone. Thus, the fluid has to change direction twice: First from rectilinear motion into circular motion, and second from circular motion into helical motion. The tangent type inlet pipe directly changes the rectilinear motion of liquid into helical motion, and therefore the overall energy loss coefficient of the hydrocyclone is smaller. The slanting pipe is designed to reduce the minor loss caused by the directional change of liquid from circular motion into helical motion, but the result shows that the energy loss coefficient increases slightly instead of decreasing. This may result from the negative influence caused by use of an unsuitable slanting angle. Ideally, the slanting angle should be the same as the spiral angle of the helical motion of liquid inside the hydrocyclone.

Fig. 7 and Table 3 show that the energy loss coefficient of the hydrocyclone decreases with the increase in length of the cylindrical part. This indicates that the frictional loss accounts for only a little of the total energy loss, because the frictional loss should be directly proportional to the distance of fluid flow. The longer the cylindrical part, the larger the space inside the hydrocyclone, and then the longer the retention time of fluid flow across the hydrocyclone; thus, the smaller the minor loss and turbulent dissipation in the hydrocyclone, and the smaller the energy loss coefficient.

In vortex finders, 30° diffuser plus cone type and 20° diffuser plus annular teeth type are both the most effective to reduce the energy loss coefficient. The main reason is that the diffuser effectively transforms the kinetic head into a pressure head, then reduces the outlet loss, and therefore the energy loss coefficient is reduced.

Compared with the conventional 20° cone with a smooth surface, the 20° cone with spiral causes the energy loss coefficient to decrease 8%. The spiral on the cone surface guides the outer helical flow and then controls the turbulent dissipation to some extent, from which lower energy loss coefficient results.

The effect of underflow pipe on the energy loss coefficient is the lowest, because the flow rate of the underflow is relatively low. Compared with the conventional straight pipe, all the measurements taken for the underflow pipe in this study result in lower energy loss coefficient. The 20° diffuser reduces the energy loss coefficient 12% by transforming the kinetic head in the underflow into a pressure head. The cone and the water-sealed tank set under the underflow pipe prevent air from entering the hydrocyclone and then hinder air core

from forming, thus the energy loss in the air core is canceled, and the energy loss coefficient is reduced.

In summary, the hydrocyclone code of optimum geometric combination that related to the lowest energy loss coefficient is A2-B3-C3-D2-E5-F5.

Pressure Structure in the Hydrocyclone with the Lowest Energy Loss Coefficient

To reveal the energy saving principles inside the hydrocyclone, the time-averaged and fluctuating characteristics of turbulent pressure in the hydrocyclone coded A2-B3-C3-D2-E5-F5 with the lowest energy loss coefficient were investigated.

Time-Averaged Characteristics of Turbulent Pressure in the Hydrocyclone with the Lowest Energy Loss Coefficient

Radial Distribution of the Pressure. The experimental radial distribution of pressure inside the hydrocyclone coded A2-B3-C3-D2-E5-F5 is shown in Fig. 9. Compared with the experimental results on the conventional hydrocyclone in the literature (3), the radial distribution illustrated in Fig. 9 is very different. In Fig. 9, the pressure in the outer helical flow reduces relatively fast

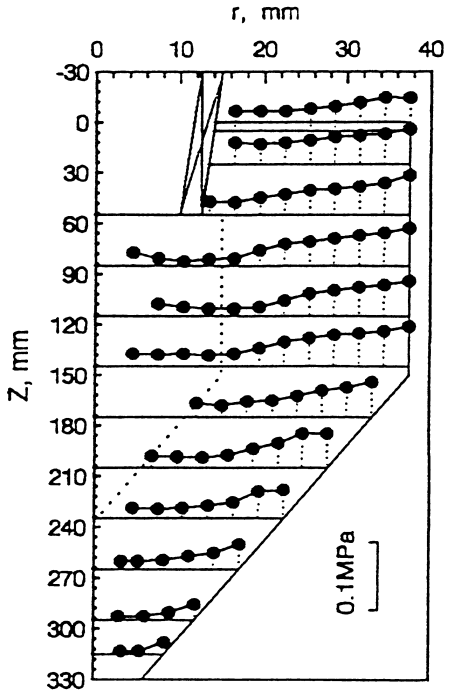

FIG. 9 Radial distribution of pressure in the hydrocyclone with low energy loss.

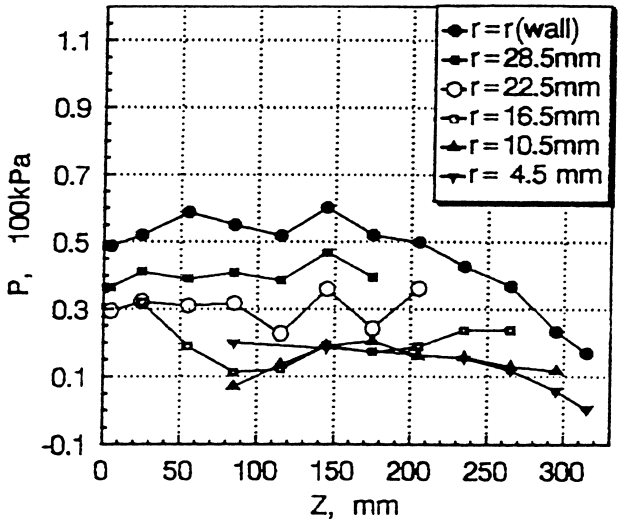

FIG. 10 Axial distribution of pressure in the hydrocyclone with low energy loss.

with decreasing radius, and reaches the minimum when the radius falls at the radial position where the outside edge of the winged core exists. In the space between the wings, pressure increases again and the radius continues to decrease. The pressure in the central space no longer reduces sharply. In the space between the wings, the velocity of liquid is hindered from increasing, and then the kinetic energy is transformed into a pressure head; therefore, both the pressure loss in the central space and the kinetic energy loss carried by the outflow are controlled effectively.

Axial Distribution of the Pressure. The axial distribution of pressure in the hydrocyclone with the lowest energy loss coefficient is shown in Fig. 10, where r(wall) is the radius of point on the inner wall of hydrocyclone. At the radial position of $r = 16.5$ mm, when the axial position increases, the pressure gradually decreases at first, reaches the minimum near the outer edge of the central winged core, and then gradually increases slightly under the winged core. At the radial position of $r = 4.5$ mm, the pressure gradually decreases when the axial position increases, and the pressures are all positive. This is very different from that in the conventional hydrocyclone shown in the literature (3).

Time-Averaged Characteristics of the Pressure Field. The three-dimensional carpet plot of time-averaged pressure in the hydrocyclone with the lowest energy loss coefficient is shown in Fig. 11. Compared with the results related to the conventional hydrocyclone shown in the literature (3), the pressure in the hydrocyclone with the lowest energy loss coefficient decreases relatively more sharply radially in the space where the radial position is larger than the radius of the outer wall of vortex finder. However, in the space where

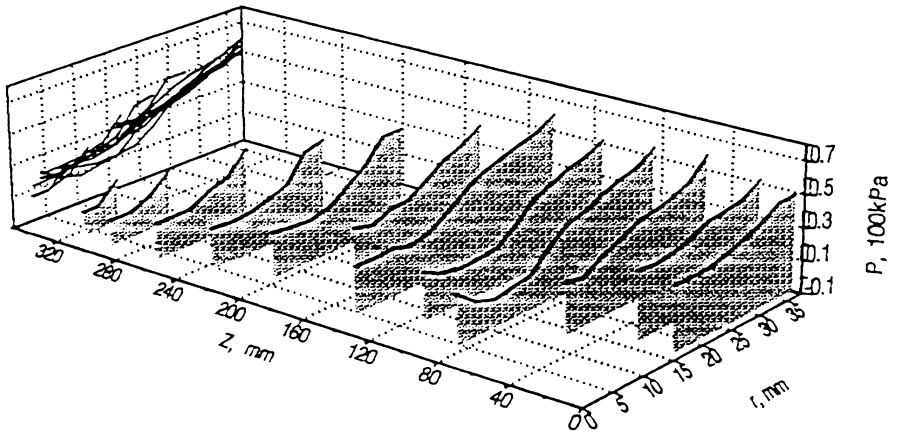

FIG. 11 Three-dimensional carpet plot of the distribution of time-averaged pressure in the hydrocyclone with low energy loss.

the radial position is smaller than the radius of the outer wall of the vortex finder, the pressure slightly increases radially instead of decreasing sharply. Thus, before the fluid in the inner helical flow enters the vortex finder, the kinetic head of the fluid has been partially transformed into a pressure head by the winged core. Therefore, not only the internal energy loss but also the outlet energy loss is reduced, and a lower energy loss coefficient results. The winged core could make a remarkable contribution to the energy saving of the hydrocyclone separation process.

Pressure Distribution at the Entrance of the Hydrocyclone. Pressure distribution at the entrance of the hydrocyclone with the lowest energy loss coefficient is shown in Fig. 12, and is different from the results of the conventional hydrocyclone shown in the literature (3). In Fig. 12, the pressure varies within a relatively large range. From point 1 to point 3, the pressure decreases because of frictional loss in the pipe. From point 3 to point 4, the fluid enters the hydrocyclone from the inlet pipe, and the pressure increases because of the sudden enlargement of the cross-sectional area of fluid flows. From point 4 to point 10, pressure generally decreases.

Fluctuating Characteristics of Turbulent Pressure in the Hydrocyclone with the Lowest Energy Loss Coefficient

Pressure Fluctuation Inside the Hydrocyclone. Fig. 13 shows the radial distribution of pressure fluctuation (PF) inside the hydrocyclone with the lowest energy loss coefficient. The results show that most PFs in the hydrocyclone are in the range of 0.8–1.3 kP_a. The general distribution law dictates that the PFs are relatively high in the spaces near the hydrocyclone wall, the outer wall of the vortex finder, and the outer edge of the winged core. The

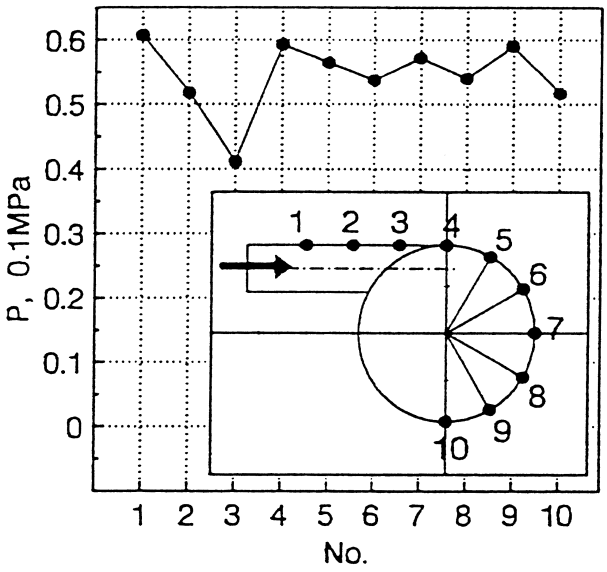

FIG. 12 Pressure variation at the entrance of the hydrocyclone with low energy loss.

PFs in the rest of the spaces are relatively low and the PF near the apex is the lowest. Compared with the experimental results related to the conventional hydrocyclone shown in the literature (3), the average dimensions of the PF in Fig. 13 are larger. In addition, in the inner helical flow near the hydrocyclone

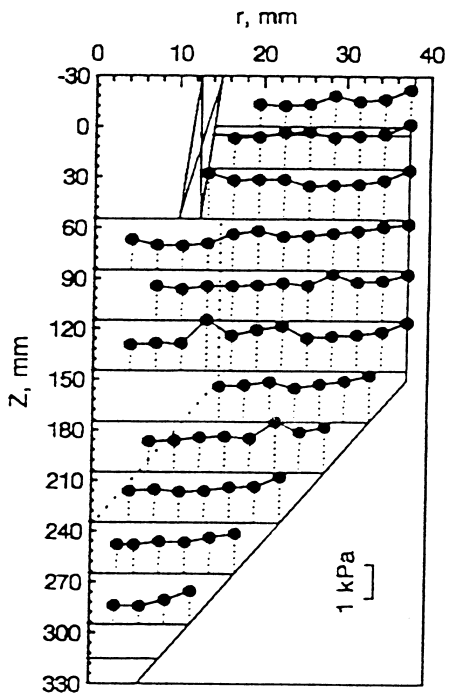

FIG. 13 Radial distribution of pressure fluctuation inside the hydrocyclone with low energy loss.

axis, the PF in Fig. 13 decreases instead of sharply increasing with the decreasing radius, which is due to the insertion of the winged core.

Relative Pressure Fluctuation Inside the Hydrocyclone. Radial distribution of the relative pressure fluctuation (RPF) inside the hydrocyclone with the lowest energy loss coefficient is shown in Fig. 14. In the space where the winged core exists, the RPF at the outer edge of the winged core is the maximum, and the RPF inside the space between the wings radially decreases with a decreasing radius. In the space outside the winged core, the RPF generally decreases slightly with an increasing radius. Compared with the results of the conventional hydrocyclone shown in the literature (3), the RPFs in the inner helical flow near the hydrocyclone axis here are effectively controlled by introducing the winged core. The RPF at some points in the central space in the conventional hydrocyclone is as large as 60% (3), whereas the maximum RPF in Fig. 14 is only about 10%. In the hydrocyclone with the lowest energy loss coefficient, the average ratio of the energy from averaged motion to the total energy in the averaged motion is much lower compared with that in the conventional hydrocyclone. This is due to the effective control of the relative pressure fluctuation in the central space. That is, the winged core could effectively control the structure of turbulence in the central space and then reduce the turbulent energy dissipation there.

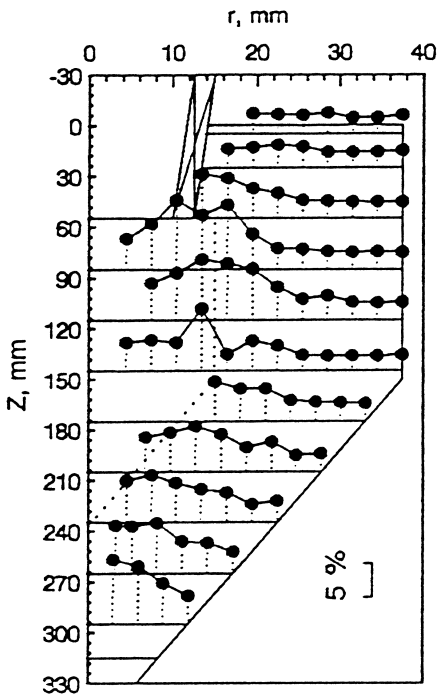

FIG. 14 Radial distribution of the relative pressure fluctuation inside the hydrocyclone with low energy loss.

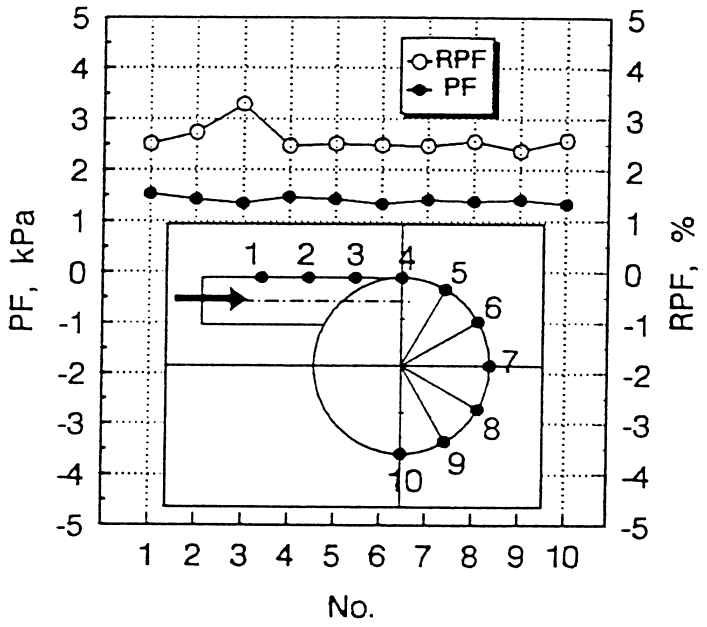

FIG. 15 Pressure fluctuation (*PF*) and relative pressure fluctuation (*RPF*) at the entrance of the hydrocyclone with low energy loss.

Pressure Fluctuation and Relative Pressure Fluctuation at the Entrance of the Hydrocyclone. The PF and RPF at the entrance of the hydrocyclone with the lowest energy loss coefficient are shown in Fig. 15. The results illustrate that the PFs at the entrance are more stable than those in the conventional hydrocyclone shown in the literature (3), and almost all of the pressure fluctuations are at the level of 1.5 kP_a, which is somewhat higher than that in the conventional hydrocyclone. The RPFs are almost maintained at the level of 2.5%, which is also somewhat higher than that in the conventional hydrocyclone. When fluid flows from test point 6 to 10, both the PF and RPF increase significantly in the conventional hydrocyclone (3), whereas those in Fig. 15 do not.

Distribution Characteristics of the Probability Density of Turbulent Pressure. The skewness coefficient, kurtosis coefficient, and the Gaussian distribution test of turbulent pressure inside the hydrocyclone with the lowest energy loss coefficient and at the entrance of the hydrocyclone are shown in Tables 4 and 5, respectively. The symbol "Yes" indicates that turbulent pressure fits the Gaussian distribution, and the symbol "No" means the contrary result. The Gaussian distribution test is carried out according to the skewness coefficient in combination with the kurtosis coefficient. Fig. 16 illustrates the Gaussian distribution test at the test levels $\alpha = 0.05$ and $\alpha = 0.01$ (7). The results in Fig. 16 show that most of the turbulent pressures inside the

TABLE 4
Skewness Coefficient (B_s), Kurtosis Coefficient (B_k), and the Gaussian Distribution (GD) Tests of the Fluctuating Pressure in the Hydrocyclone with Low Energy Loss

		Z (mm)										
r (mm)	Parameter	5	25	55	85	115	145	175	205	235	265	295
37.5	B_s	0.049	0.059	0.016	0.042	0.087	–0.058					
	B_k	1.635	1.547	1.445	1.566	1.724	1.493					
	GD	No	No	No	No	No	No					
34.5	B_s	0.033	0.030	0.041	–0.015	–0.011	–0.014	–0.051				
	B_k	1.633	1.698	1.480	1.633	1.582	1.532	1.460				
	GD	No	No	No	No	No	No	No				
31.5	B_s	–0.017	0.095	0.045	–0.020	0.016	0.027	0.068				
	B_k	1.716	1.692	1.474	1.556	1.716	1.492	1.467				
	GD	No	No	No	No	No	No	No				
28.5	B_s	–0.169	–0.043	–0.028	–0.007	0.071	0.025	–0.083	0.043			
	B_k	2.337	1.474	1.626	1.593	2.220	1.519	1.515	1.463			
	GD	Yes	No	No	No	Yes	No	No	No			
25.5	B_s	–0.185	0.058	–0.007	0.089	0.030	0.034	0.030	0.013			
	B_k	2.062	2.187	1.584	1.712	1.603	1.624	1.540	1.500			
	GD	Yes	Yes	No	No	No	No	No	No			

22.5	B_s	0.017	–0.015	–0.142	0.067	0.036	0.087	0.029	0.611	0.019		
	B_k	1.718	2.152	1.854	1.638	1.624	1.815	1.458	3.372	1.450		
	GD	No	Yes	No	No	No	No	No	Yes	No		
19.5	B_s	0.152	–0.017	0.051	0.038	0.028	0.056	–0.054	0.008	0.054	-0.002	
	B_k	1.886	1.608	1.705	1.637	1.667	1.709	1.586	1.606	1.511	1.490	
	GD	No	No	No	No	No	No	No	No	No	No	
16.5	B_s		–0.003	0.049	–0.049	0.002	0.076	0.026	0.055	0.112	0.087	
	B_k		1.591	1.634	1.857	1.519	1.627	1.504	1.568	1.794	1.942	
	GD		No	No	No	No	No	No	No	No	Yes	
13.5	B_s			–0.367	–0.027	0.022	–0.187		–0.036	0.051	–0.045	–0.108
	B_k			2.617	1.629	1.599	2.323		1.536	1.482	1.587	1.910
	GD			Yes	No	No	Yes		No	No	No	No
10.5	B_s				0.036	0.020	–0.020		0.069	0.042	0.170	0.012
	B_k				1.776	1.695	1.627		1.683	1.546	2.186	1.576
	GD				No	No	No		No	No	Yes	No
7.5	B_s				–0.008	0.126	0.085		–0.007	–0.024	–0.068	0.100
	B_k				1.944	1.994	1.854		1.578	1.552	1.541	2.195
	GD				Yes	Yes	No		No	No	No	Yes
4.5	B_s				0.032		0.044			0.060	–0.001	0.098
	B_k				1.777		1.654			1.626	1.573	2.209
	GD				No		No			No	No	Yes

TABLE 5
Skewness Coefficient (B_s), Kurtosis Coefficient (B_k), and the Gaussian Distribution (GD) Tests of the Fluctuating Pressure at the Entrance of Hydrocyclone with Low Energy Loss

No.	1	2	3	4	5	6	7	8	9	10
B_s	–0.028	–0.016	–0.067	–0.001	0.025	–0.004	–0.007	–0.019	–0.017	0.030
B_k	1.504	1.438	1.528	1.507	1.470	1.514	1.461	1.564	1.440	1.464
GD	No	No	No	No	No	No	No	No	No	No

hydrocyclone with low energy loss and at the entrance of the hydrocyclone do not fit the Gaussian distribution at the test level $\alpha = 0.01$, and that only at a few positions do the turbulent pressures fit a Gaussian distribution at the test level $\alpha = 0.05$. The Gaussian distribution tests in Tables 4 and 5 are carried out at the test level $\alpha = 0.01$.

Tables 4 and 5 show that most of the turbulent pressures do not fit a Gaussian distribution, which is mainly because the kurtosis coefficients are all fairly small. The above results illustrate two facts: (*a*) The average PF in the hydrocyclone with the lowest energy loss coefficient is relatively large, which indicates that the turbulent energy dissipation in the space outside the inner helical flow area is the minor composition part of the total energy loss; and (*b*) The turbulent fine-structure intermittency (16, 17) exists at the most positions in the hydrocyclone coded A2-B3-C3-D2-E5-F5.

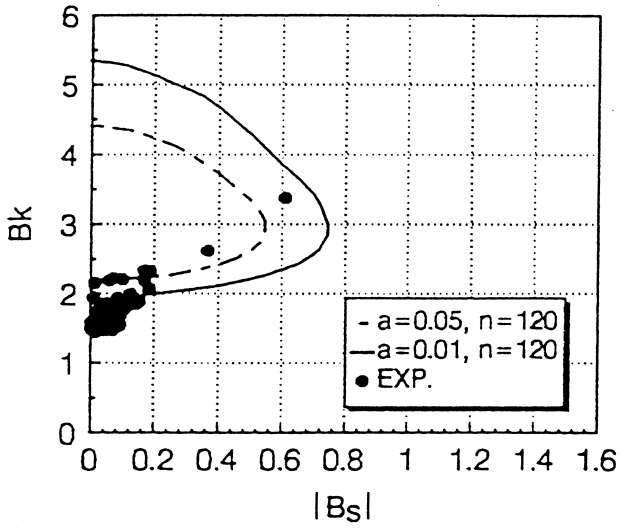

FIG. 16 Gaussian distribution test of the fluctuating pressure inside and at the entrance of the hydrocyclone with low energy loss.

Energy Saving Principles and Measures

Principles

From the investigation mentioned above and a series of previous investigations (1–3), some energy saving principles could be concluded as follows:

1. To reduce the inlet energy loss, the main principle is controlling the minor loss which is due to the directional change of fluid and the eddies.
2. To effectively reduce the total energy loss, remove all of the turbulent loss, kinetic head loss, and frictional loss in the air core by eliminating the air core.
3. The inner helical flow area near the hydrocyclone axis subject to significant energy loss. Effective control of the turbulent loss and the minor loss, which are due to the acceleration of fluid in this area, could result in a notable reduction of the total energy loss in the hydrocyclone separation process.
4. The turbulent loss, frictional loss, and minor loss in the spaces, excepting those spaces mentioned above (in items 1, 2, and 3), make relatively small contributions to the total energy loss.
5. The kinetic head loss with the outflow of the conventional hydrocyclone makes a notable contribution to the total energy loss. Therefore, it is essential for the recovery of partial kinetic head and the reduction of the total energy loss to partially transform the kinetic head in the outflow into the pressure head.
6. The total energy loss could be reduced by decreasing the pressure head loss carried by the outflow. This results from the reduction of the outflow pressure level, which must be maintained to ensure that smooth outflow flows out of the hydrocyclone.

Measures

1. To reduce the inlet loss of the hydrocyclone, it is essential to consider the problem from the overall viewpoint instead of focusing on the local situation, i.e., the target parameter should be the total energy loss of the hydrocyclone rather than merely the inlet loss. The experimental results show that the tangent type pipe is the best inlet pipe for the reduction of the total energy loss.
2. There are many methods to eliminate the air core, such as introducing a winged core, central solid core, or central cone inside the hydrocyclone, and attaching the solid cone or water-sealed tank to the underflow pipe. The winged core results in the most notable effect on the reduction of the total energy loss.
3. Both central solid core and winged core are effective in reducing the turbulent loss and the minor loss in the inner helical flow area near the hy-

drocyclone axis that is due to the acceleration of fluid, in which the overall function of the winged core is much more efficient.

4. To further reduce energy loss in the spaces, in addition to the methods mentioned in measures 1, 2, and 3, some possible effective measures are to increase the length of the cylindrical part of hydrocyclone, or introduce spirals to the inner wall of the cone part.
5. There are two main measures to reduce the kinetic head loss in the outflow. The first is to take curved diffusers as a vortex finder and as an underflow pipe, and therefore partially transform the kinetic head into a pressure head in the outlet pipes. The second measure is to insert a winged core in the central area of the hydrocyclone to let the transformation of energy from the kinetic head into the pressure head take place before the outflow enters the vortex finder. The combination of these measures could result in notable recovery of the kinetic head carried by the outflow.
6. There are many measures to reduce the pressure level needed for the smooth outflow of the hydrocyclone. For example, the use of curved diffusers as vortex finder and underflow pipe, insertion of inner diffuser into the vortex finder, and attachment of a siphon or vacuum device to the outlet of vortex finder. Of these methods, the measure that uses curved diffusers as vortex finder and underflow pipe is the best choice because both the overall energy saving function and the structural simplification are considered.

CONCLUSIONS

The effect of structure of flow field on the energy consumption was investigated systematically. The degree of influence of the structural factors on the energy loss coefficient can be put in order from higher to lower as follows: central inserted parts $>$ inlet pipes $>$ cylindrical parts $>$ vortex finders $>$ cone parts $>$ underflow pipes. In the central inserted parts, the winged core is the best location for reducing the energy loss. The optimum geometric combination of the hydrocyclone related to the lowest energy loss coefficient is coded as A2-B3-C3-D2-E5-F5.

The turbulent pressure structure in the hydrocyclone with the lowest energy loss coefficient, including all of the time-averaged characteristics and fluctuating characteristics, is very different from that in the conventional hydrocyclone, and the difference is especially large in the inner helical flow area near the hydrocyclone axis. The energy saving mechanisms in the hydrocyclone were examined by comparing and analyzing the differences in these characteristics.

The energy saving principles and relevant effective measures for hydrocyclones were proposed systematically and discussed.

NOMENCLATURE

A1	involute type inlet pipe
A2	tangent type inlet pipe
A3	arc type inlet pipe
A4	slanting pipe inlet pipe
A5	spiral type inlet pipe
B1	vortex finder being straight pipe with thin wall
B2	vortex finder being straight pipe with thick wall
B3	vortex finder being 30° diffuser plus cone
B4	vortex finder being 20° diffuser plus annular teeth
B5	vortex finder being straight pipe with thin wall plus siphon
B_k	kurtosis coefficient
B_s	skewness coefficient
C1	parabola type cone part
C2	hyperbola type cone part
C3	cone part, 20° cone with spiral
C4	cone part, 20° cone with rings
C5	cone part, 20° cone with smooth surface
D	hydrocyclone diameter
D1	underflow pipe being straight pipe
D2	underflow pipe being 20° diffuser
D3	underflow pipe being 30° diffuser plus cone
D4	underflow pipe being straight pipe plus cone
D5	underflow pipe being straight pipe plus water-sealed tank
d_e	inlet diameter of hydrocyclone
E1	without inserted part
E2	central inserted part, solid core
E3	central inserted part, central cone
E4	central inserted part, inner diffuser
E5	central inserted part, winged core
$(Eu)_c$	cyclone characteristic Euler number
$(Eu)_e$	inlet characteristic Euler number
F1	length of cylindrical part, 0.4 D
F2	length of cylindrical part, 0.8 D
F3	length of cylindrical part, 1.2 D
F4	length of cylindrical part, 1.6 D
F5	length of cylindrical part, 2.0 D
$(Fr)_c$	cyclone characteristic Froude number
g	gravitational acceleration
GD	gaussian distribution test
K	energy loss coefficient

P_e	inlet pressure
PF	pressure fluctuation
Q_e	capacity of hydrocyclone
r	radial position
$(Re)_c$	cyclone characteristic Reynolds number
RPF	relative pressure fluctuation
v	hydrocyclone characteristic velocity
v_e	inlet velocity of liquid
Z	axial position
μ	viscosity of liquid
ρ	density of liquid

ACKNOWLEDGMENT

This research was supported by China Postdoctoral Science Foundation and by the Doctoral Science Foundation of State Educational Ministry of China.

REFERENCES

1. L.-Y. Chu, X.-Z. Lee, and W.-M. Chen, "Energy Consumption and its Reduction in Hydrocyclone Separation Process Part I: Theoretical Investigations of Pressure Distribution and Energy Consumption Mechanism in Hydrocyclones," in Proceedings 7th World Filtration Congress, Budapest, Hungary, May 1996, Vol. I, pp. 152–156.
2. L.-Y. Chu, W.-M. Chen, X.-Z. Lee, and C.-G. Wu, "Numerical Simulation of Turbulence and Structure of Turbulence in Hydrocyclones," *Transactions of Nonferrous Metals Society of China* (English ed.), *9*(1), 128–136 (1999).
3. L.-Y. Chu, J.-J. Qin, W.-M. Chen, and X.-Z. Lee, "Energy Consumption and its Reduction in Hydrocyclone Separation Process. Part II: Time-averaged and Fluctuating Characteristics of the Turbulent Pressure in a Hydrocyclone," *Sep. Sci. Technol.*, *35*(15), 2543–2560 (2000).
4. L.-Y. Chu and Q. Luo, "Hydrocyclone with High Sharpness of Separation," *Filtr. and Sep.*, *31*(7), 733–736 (1994).
5. L.-Y. Chu, W.-M. Chen, and Q. Luo, "Separation Characteristics in the Hydrocyclone with a Central Cone and Annular Teeth," *Transactions of Nonferrous Society of China* (English ed.), *6*(4), 11–15 (1996).
6. J. R. Xu, Research on the forced vortex and internal loss in hydrocyclones, Ph.D. Dissertation, Northeast Institute of Technology, Shenyang, China, 1989.
7. F. S. Ma, L. C. He, and M. S. Yu, *Applied Probability Statistics*, Higher Education Press, Beijing, 1989.
8. G. Z. Liu, *Principles and Analyzing Methods of Fluid Mechanics*, Higher Education Press, Beijing, 1992.
9. L. Svarovsky, *Solid-Liquid Separation* (3rd ed.), Butterworth & Co. Ltd., London, 1990.
10. A. Sahlin, A. V. Johannson, and P. H. Alfredsson, "The Possibility of Drag Reduction by Outer Layer Manipulators in Turbulent Boundary Layers," *Phys. Fluids*, *31*(10), 2814–2820 (1988).
11. R. Falco, "Correlation of Outer and Passive Wall Region Manipulation with Boundary Layer Coherent Structure Dynamics of Suggestions for Improved Devices," *Am. Inst. Aeronaut. Astronaut.* 89–1026, 1989.

12. J. R. Xu and Q. Luo, "Forced Vortex and Hydrocyclone," *Mining Metal. Eng., 9*(2), 29–33 (1989).
13. J. D. Boadway, "A Hydrocyclone with Recovery of Velocity Energy," in Proceedings 2nd International Conference on Hydrocyclones, Bath, England, Sept. 1984, pp. 99–108.
14. Y. H. Yuan and B. Y. Wang, "The Development Situation of Hydrocyclones," *Mining and Metal. Eng., 3*(3), 62–67 (1983).
15. W. A. Gong, "Design and Calculation of the Hydrocyclone Volute," *China Petrol. Machinery, 20*(12), 1–6 (1992).
16. F. Hu, *Turbulence, Intermittency and Boundary Layer of Atmosphere*, Science Press, Beijing, 1995.
17. W. D. McComb, *The Physics of Fluid Turbulence*, Clarendon Press, Oxford, 1990.

Received by editor November 9, 1999
Revision received March 2000